

Analytic Computational Method for Solving Fractional Nonlinear Equations in Magneto-Acoustic Waves

RANIA SAADEH
Department of Mathematics
Zarqa University
Zarqa 13110,
JORDAN

Abstract: - In this article, we employ a useful and intriguing method known as the ARA-homotopy transform approach to explore the fifth-order Korteweg-de Vries equations that are nonlinear and time-fractional. The study of capillary gravity water waves, magneto-sound propagation in plasma, and the motion of long waves under the effect of gravity in shallow water have all been influenced by Korteweg-de Vries equations. We discuss three instances of the fifth-order time-fractional Korteweg-de Vries equations to demonstrate the efficacy and applicability of the proposed method. Utilizing, also known as the auxiliary parameter or convergence control parameter, the ARA-homotopy transform technique which is a combination between ARA transform and the homotopy analysis method, allows us to modify the convergence range of the series solution. The obtained results show that the proposed method is very gratifying and examines the complex nonlinear challenges that arise in science and innovation.

Key-Words: - *Nonlinear fractional partial differential equation, ARA-Homotopy transform method, ARA transform, Caputo derivative.*

Received: May 23, 2022. Revised: October 25, 2022. Accepted: December 3, 2022. Published: December 31, 2022.

1 Introduction

Plasma is typically regarded as a unique phase of matter in physics and lacks a fixed shape or volume. By heating a neutral gas or exposing it to a desired electromagnetic field, which causes an ionized gaseous material to become more electrically conductive, plasma can be created. Because of the free electric charges that make the plasma electrically conductive, the plasma reacts strongly to electromagnetic fields. Thus, electric and/or magnetic forces would dominate its characteristics. The matter in the plasma state is referred to as some forms of flame, stars, and the Sun's corona. The realm of intensity production is where plasmas are most practically utilized. A crucial method for producing electricity is to use heat sources to turn water into steam, which drives turbo generators. Unsettling effects that are compressible propagate through plasma as magneto-acoustic waves that are fueled by both gas pressure and attractive force. Particle nonpartisan effects have a role in the partial coupling of ionized plasmas, the constituents of

ionized and impartial species. As a result, in the presence of low magnetic field and low temperature, the magneto-acoustic wave persists as particle acoustic waves and Alfvén waves, respectively. The heating of the solar corona is significantly influenced by the magneto-acoustic waves [1], [2], [3], [4].

The phenomenon of nonlinear equations describes the fundamental physical aspects in nature ranging from chaotic behaviour in biological systems [2], plasma physics - plasma containment in stellarators, and tokamaks to energy generation. [3], [4], quantum mechanics, [5], nonlinear optics, [6], solid-state physics and up to fibre optical communication devices, [7], dual wave soliton solution, [8], unidirectional shallow water waves [9], analytical wave solutions, [10], unmagnetized dust plasma, [11], optimal solitons for the nonlinear dynamics, [12]. The various phenomena of nonlinear equations are modelled in terms of many orders of nonlinear partial differential equations, [13], [14], [15], [16], [17]. Partial differential equations are largely utilised to represent physical

systems, but unfortunately, many of them don't have the exact solution. Moreover, the accurate solution to this nonlinear phenomenon is not available in the literature and hence to solve these nonlinear systems, there is an essence of studying the nonlinear phenomena with appropriate and more efficient methods.

Since the solution of the KdV equation can be explained exactly and precisely, it is predominantly distinguished as the archetypal illustration of an exactly solvable model, [18], [19], [20]. The KdV equation amalgamates dispersion and nonlinearity and provides stationary solutions tracing both periodic and solitary waves. It represents a model for the interpretation of long waves which are weakly nonlinear with small dispersion in media. Subsequently, various kinds of KdV equations possess many remarkable properties and are being considered as a model to explain the wide range of physical phenomena which exist in the connected branches of mathematics and physics.

There are various analytical and numerical methods available for handling various forms of fifth-order KdV-type equations in the literature. Some of them are the Adomian decomposition technique, Modified Adomian Decomposition Method, Laplace decomposition approach, Hyperbolic and exponential ansatz methods, Multiple Exp-function method, and others [30-33].

In the present investigation, we consider the time-fractional fifth-order KdV equations with initial conditions as follows, [18]:

$${}^c u(x, t) + u_x + u^2 u_{xx} + u_x u_{xx} - u^2 u_{xxx} + u_{xxxxx} = 0, \quad (1)$$

with the initial condition $u(x, 0) = \frac{1}{x}$.

$$D_t^\alpha u(x, t) + uu_x - uu_{xxx} + u_{xxxxx} = 0, \quad (2)$$

with initial conditions $u(x, 0) = e^x$.

$$D_t^\alpha u(x, t) + uu_x + u_{xxx} - u_{xxxxx} = 0, \quad (3)$$

with initial conditions $u(x, 0) = \frac{105}{169} \operatorname{sech}^4\left(\frac{x-k}{2\sqrt{13}}\right)$.

Here, $0 < \alpha \leq 1$, Eqs. (3) and (4) are called fifth-order KdV equations and Equation (5) is called the Kawahara equation [38].

The KdV equations (3) and (4) are crucial for explaining how long waves move in shallow water when there is gravity. In order to study the propagation of oscillatory solitary waves in a dispersive medium, Kuwahara first applied the Kawahara equation (5) in 1972, [38]. The above equations describe the interaction between nonlinearity and dispersion in the theoretically simplest terms possible. The higher order nonlinear factors that are present in the equations under

consideration express higher amplitude internal waves.

Now, the solutions for the above-mentioned equations have been investigated by employing a new computational technique, known as ARA-homotopy transform method (or briefly, ARA-HTM). The considered technique is a graceful unification of the homotopy algorithm and ARA transform [34], [35], [36], [38].

The proposed technique gives a great degree of freedom in picking initial approximations and auxiliary linear operators; as a result, the complexity of the problem can be reduced by transforming it into an infinitely countable number of easier, linear subproblems, helping in reducing the time of computational work.

Following that, the article's remaining portion is decorated as: The fundamental and standard definitions of the fractional derivatives, and the basic idea of ARA transform of Caputo fractional derivative is presented in section 2. The methodology of the considered analytical technique for nonlinear fractional partial differential equations can be seen in Section 3. The investigation of the considered problem along with the incorporation of their graphical results using projected technique is done in section 4. Section 5 cites the description about the obtained results. Section 6 is decorated with the concluding remarks followed by the references.

2 Basic Facts and Theorems

The basic definitions of fractional operators and the ARA transform, which are related to this study, are presented in this section of this research.

Definition 1. The Caputo fractional derivative of order α of the function $u \in C_{-1}^n$ is defined as

$$D^\alpha u(x) = \begin{cases} \frac{d^n u(x)}{dx^n}, & \alpha = n \in \mathbb{N}, \\ \frac{1}{\Gamma(n-\alpha)} \int_0^x (x-\vartheta)^{n-\alpha-1} u^{(n)}(\vartheta) d\vartheta, & n-1 < \alpha < n, n \in \mathbb{N}. \end{cases} \quad (4)$$

Definition 2. [37] If $u(x)$ is a continuous function on the interval $(0, \infty)$, then ARA transform of order n of is defined by

$$\mathcal{G}_n[u(x)](s) = s \int_0^\infty x^{n-1} e^{-sx} u(x) dx, s > 0. \quad (5)$$

We define the inverse ARA transform as follows

$$u(x) = \frac{(-1)^n}{2\pi i} \int_{c-i\infty}^{c+i\infty} e^{sx} \left((-1)^n \left(\frac{1}{s\Gamma(n-1)} \int_0^s (s-v)^{n-2} \mathcal{G}_{n+1}[u(v)](v) dv + \sum_{k=0}^{n-1} \frac{s^k}{k!} \frac{\partial^k U(0)}{\partial s^k} \right) \right) ds,$$

where $c = \text{Re}(s)$ and

$$U(s) = \int_0^\infty e^{-sx} u(x) dx.$$

Now, we introduce some basic properties of ARA transform that are important in our study.

Assume that $u(x)$ and $w(x)$ are two continuous functions defined on the interval $(0, \infty)$ such that ARA transform exists, then for $s > 0$, we have

- $\mathcal{G}_n[au(x) + bw(x)](s) = a\mathcal{G}_n[u(x)](s) + b\mathcal{G}_n[g(x)](s)$, where a and b are two constants.

- $\lim_{s \rightarrow \infty} \mathcal{G}_1[u(x)](s) = u(0)$.

- $\mathcal{G}_1[u'(x)](s) = s\mathcal{G}_1[u(x)](s) - su(0)$. (6)

- $\mathcal{G}_1[x^\alpha](s) = \frac{\Gamma(\alpha+1)}{s^\alpha}, s > 0, \alpha > 0$. (7)

- $\mathcal{G}_1[D^\alpha u(x)](s) = \frac{1}{s^{m-\alpha}} \mathcal{G}_1[u^{(m)}(x)](s)$,
 $m - 1 < \alpha \leq m$. (8)

Remark 1. In this study, we focus the proposed method on ARA transform of order 1, to simplify the notation, we use \mathcal{G} instead of \mathcal{G}_1 to denote ARA transform.

3 The basic idea of the ARA-HTM

To illustrate the main idea of ARA-HTM, let us consider the following time fractional PDE

$$D_t^\alpha g(x, t) + L(g(x, t)) + N(g(x, t)) = r(x, t), \quad n - 1 < \alpha \leq n, \quad (9)$$

where $D_t^\alpha g(x, t)$ cites the α Caputo fractional derivative of the function $g(x, t)$, $r(x, t)$ denotes the source term, linear and nonlinear differential operators are represented by L and N respectively.

Now, hiring ARA transform \mathcal{G}_t with respect to the variable t , to Eq.(9) and using the properties of ARA to the fractional derivative, we conclude

$$s^\alpha \mathcal{G}_t[u(x, t)] - \sum_{k=0}^{n-1} s^{\alpha-k} u^{(k)}(x, 0) + \mathcal{G}_t[L(u(x, t))] + \mathcal{G}_t[N(u(x, t))] = \mathcal{G}_t[r(x, t)]. \quad (10)$$

Simplifying Eq.(10), we have

$$\mathcal{G}_t[u(x, t)] - \frac{1}{s^\alpha} \sum_{k=0}^{n-1} s^{\alpha-k} u^{(k)}(x, 0) + \frac{1}{s^\alpha} \{\mathcal{G}_t[L(u(x, t))] + \mathcal{G}_t[N(u(x, t))]\} - \mathcal{G}_t[r(x, t)] = 0. \quad (11)$$

The nonlinear operator N with HAM can be expressed as

$$N[\varphi(x, t; q)] = \mathcal{G}_t[\varphi(x, t; q)] - \frac{1}{s^\alpha} \sum_{k=0}^{n-1} s^{\alpha-k} \varphi^{(k)}(x, t; q)(0^+) + \frac{1}{s^\alpha} \{\mathcal{G}_t[L(\varphi(x, t; q))]\} + \mathcal{G}_t[N(\varphi(x, t; q))] - \mathcal{G}_t[r(x, t)], \quad (12)$$

where $\varphi(x, t; q)$ is a real valued function of x, t and q and $q \in [0, \frac{1}{n}]$.

The zeroth order deformation equation involving the auxiliary function $H(x, t)$ is as follows:

$$(1 - nq)\mathcal{G}_t[\varphi(x, t; q) - u_0(x, t)] = \hbar q H(x, t) N[\varphi(x, t; q)], \quad (13)$$

where $\hbar \neq 0$ is the convergence control parameter, $q \in [0, \frac{1}{n}]$ ($n \geq 1$) is the embedding parameter, $u_0(x, t)$ is an initial guess of $u(x, t)$, $\varphi(x, t; q)$ is a function to be determined. The below equations justify for $q = 0$ and $q = \frac{1}{n}$.

$$\varphi(x, t; 0) = u_0(x, t), \quad \varphi(x, t; \frac{1}{n}) = u(x, t), \quad (14)$$

respectively. As we move q from 0 to $\frac{1}{n}$, the solution $\varphi(x, t; q)$ converges from $u_0(x, t)$ to the solution $u(x, t)$. After operating, the Taylor theorem for the function $\varphi(x, t; q)$ around q leads to

$$\varphi(x, t; q) = u_0(x, t) + \sum_{m=1}^\infty u_m(x, t) q^m, \quad (15)$$

where

$$u_m(x, t) = \frac{1}{m!} \frac{\partial^m \varphi(x, t; q)}{\partial q^m} \Big|_{q=0}. \quad (16)$$

On choosing the appropriate the auxiliary parameter \hbar , the initial guess $u_0(x, t)$ and $H(x, t)$, the auxiliary linear operator, the series (15) converges at $q = \frac{1}{n}$, which leads to one of the solutions of the original nonlinear equation of the form

$$u(x, t) = u_0(x, t) + \sum_{m=1}^\infty u_m(x, t) (\frac{1}{n})^m. \quad (17)$$

Next, the m^{th} order deformation equation obtained by differentiating the zeroth order deformation equation m -times followed by dividing the resulting equation by $m!$ at $q = 0$ leads to

$$\mathcal{G}_t[u_m(x, t) - K_m u_{m-1}(x, t)] = \hbar H(x, t) \mathfrak{R}_m(\vec{u}_{m-1}), \quad (18)$$

and the vector \vec{u}_m is demonstrated as

$$\vec{u}_m = \{u_0(x, t), u_1(x, t), \dots, u_m(x, t)\}. \quad (19)$$

The following recursive is obtained by hiring the inverse ARA transform to Eq.(18) as

$$u_m(x, t) = K_m u_{m-1}(x, t) + \hbar \mathcal{G}_t^{-1}[H(x, t) \mathfrak{R}_m(\vec{u}_{m-1})], \quad (20)$$

where

$$\mathfrak{R}_m(\vec{u}_{m-1}) = \frac{1}{(m-1)!} \frac{\partial^{m-1} N[\varphi(x, t; q)]}{\partial q^{m-1}} \Big|_{q=0}, \quad (21)$$

and

$$K_m = \begin{cases} 0, & m \leq 1, \\ n, & m > 1. \end{cases} \quad (22)$$

Lastly, the terms of the ARA-HTM series solution are attained by evaluating Eq.(20).

4 Numerical Simulations

The investigation of the following examples proves the efficiency and applicability of the presented scheme.

Problem 4.1.

The fifth-order time-fractional KdV equation defined in Equation (3)

$$D_t^\alpha u(x, t) + u_x + u^2 u_{xx} + u_x u_{xx} - 20u^2 u_{xxx} + u_{xxxxx} = 0, \quad (23)$$

with the initial condition

$$u(x, 0) = \frac{1}{x}. \quad (24)$$

Introduce ARA transform in Eq.(23) along with the starting solution in Eq.(24), leads to

$$\mathcal{G}_t[u(x, t)] - \frac{1}{s} \left\{ \frac{1}{x} \right\} + \frac{1}{s^\alpha} \mathcal{G}_t \left\{ \frac{\partial u}{\partial x} + u^2 \frac{\partial^2 u}{\partial x^2} + \frac{\partial u}{\partial x} \frac{\partial^2 u}{\partial x^2} - 20u^2 \frac{\partial^3 u}{\partial x^3} + \frac{\partial^5 u}{\partial x^5} \right\} = 0. \quad (25)$$

The nonlinear operator N is defined as follows

$$N[\varphi(x, t; q)] = \mathcal{G}_t[\varphi(x, t; q)] - \frac{1}{s} \left\{ \frac{1}{x} \right\} + \frac{1}{s^\alpha} \mathcal{G}_t \left\{ \frac{\partial \varphi(x, t; q)}{\partial x} + \varphi^2(x, t; q) \frac{\partial^2 \varphi(x, t; q)}{\partial x^2} + \frac{\partial \varphi(x, t; q)}{\partial x} \frac{\partial^2 \varphi(x, t; q)}{\partial x^2} - 20\varphi^2(x, t; q) \frac{\partial^3 \varphi(x, t; q)}{\partial x^3} + \frac{\partial^5 \varphi(x, t; q)}{\partial x^5} \right\}. \quad (26)$$

The m^{th} order deformation equation is

$$\mathcal{G}_t[u_m(x, t) - K_m u_{m-1}(x, t)] = \hbar \mathfrak{R}_m[\vec{u}_{m-1}], \quad (27)$$

where

$$\begin{aligned} \mathfrak{R}_m[\vec{u}_{m-1}] = & \mathcal{G}_t[u(x, t)] - \left(1 - \frac{K_m}{n}\right) \frac{1}{s} \left\{ \frac{1}{x} \right\} \\ & + \frac{1}{s^\alpha} \mathcal{G}_t \left\{ \frac{\partial u_{m-1}}{\partial x} + \sum_{j=0}^i \sum_{i=0}^{m-1} u_j u_{i-j} \frac{\partial^2 u_{m-1-i}}{\partial x^2} + \sum_{i=0}^{m-1} \frac{\partial u_i}{\partial x} \frac{\partial^2 u_{m-1-i}}{\partial x^2} - 20 \sum_{j=0}^i \sum_{i=0}^{m-1} u_j u_{i-j} \frac{\partial^3 u_{m-1-i}}{\partial x^3} + \frac{\partial^5 u_{m-1}}{\partial x^5} \right\}. \end{aligned} \quad (28)$$

On implementing inverse ARA transform on Eq.(24), we get

$$u_m(x, t) = K_m u_{m-1}(x, t) + \hbar \mathcal{G}_t^{-1} \{ \mathfrak{R}_m[\vec{u}_{m-1}] \}. \quad (29)$$

Solving the above equations consistently gives

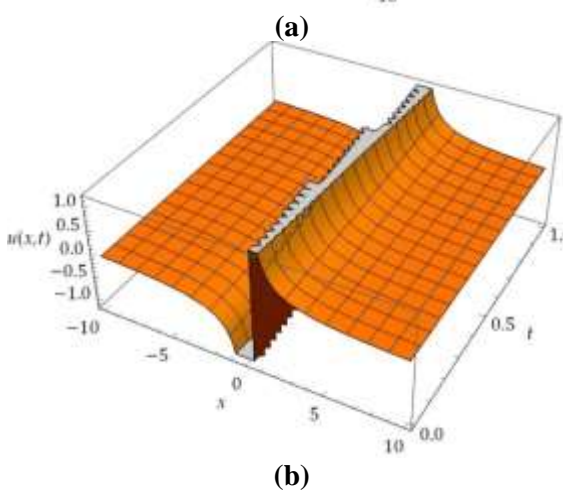
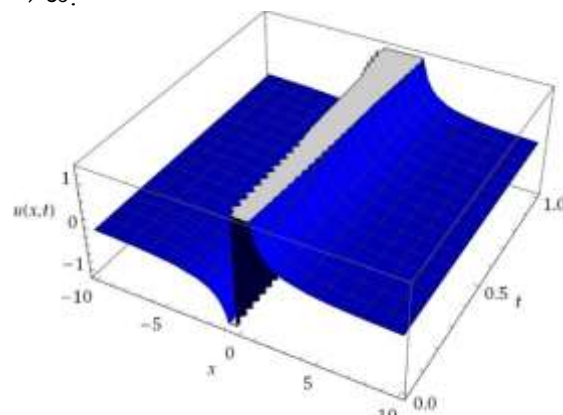
$$u_0(x, t) = \frac{1}{x},$$

$$\begin{aligned} u_1(x, t) &= \frac{\hbar t^\alpha}{\Gamma[\alpha+1]} \left(-\frac{1}{x^2} \right), \\ u_2(x, t) &= \frac{(n+\hbar)\hbar t^\alpha}{\Gamma[\alpha+1]} \left(-\frac{1}{x^2} \right) + \frac{2t^{2\alpha}\hbar^2}{x^3\Gamma[2\alpha+1]}, \\ u_3(x, t) &= \frac{(n+\hbar)^2\hbar t^\alpha}{\Gamma[\alpha+1]} \left(-\frac{1}{x^2} \right) + \frac{2(n+\hbar)t^{2\alpha}\hbar^2}{x^3\Gamma[2\alpha+1]} - \frac{2t^{3\alpha}\hbar^3((1080+2x+3x^4)\Gamma[1+\alpha]^2 - (540+x)\Gamma[2\alpha+1])}{x^8\Gamma[\alpha+1]^2\Gamma[3\alpha+1]}, \end{aligned}$$

Finally, after getting further iterative terms, the essential series solution of Eq.(23) is presented by

$$u(x, t) = u_0(x, t) + \sum_{m=1}^{\infty} u_m(x, t) \left(\frac{1}{n} \right)^m. \quad (30)$$

By taking $\alpha = 1, \hbar = -1$ and $n = 1$, then the obtained solution $\sum_{m=1}^N u_m(x, t) \left(\frac{1}{n} \right)^m$, converges to the exact solution $u(x, t) = \frac{1}{x-t}$ of the Eq.(23), as $N \rightarrow \infty$.



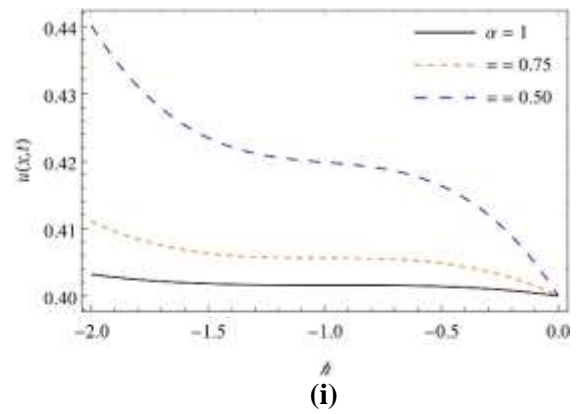
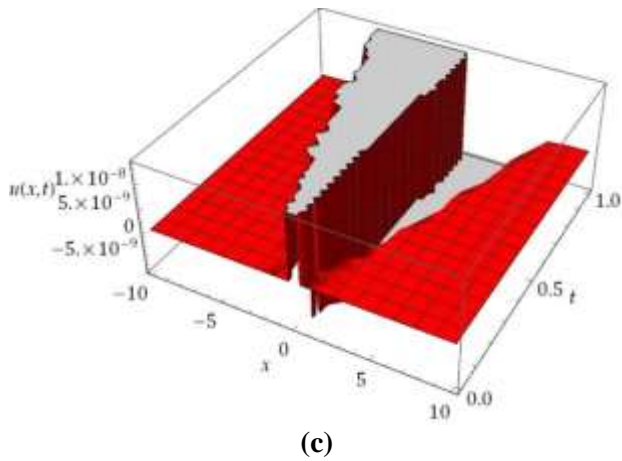


Figure 1. (a) 3D plot for ARA-HTM solution, (b) surface of exact solution, (c) approximate solution surface at $\alpha = 1, n = 1$ and $\hbar = -1$ for Problem 4.1.

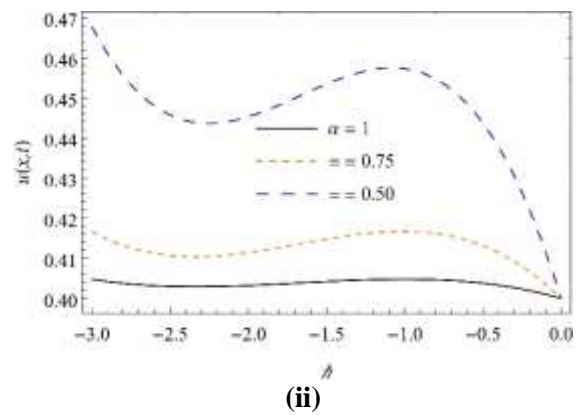
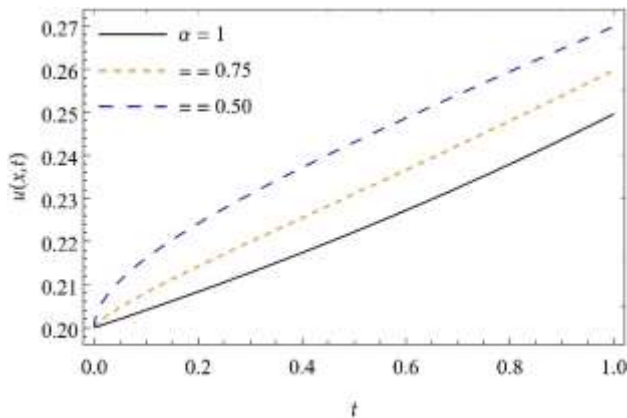


Figure 2. $u(x, t)$ with versus t for Problem 4.1 when $\hbar = -1, x = 5$ and $n = 1$ for distinct values of α .

Figure 3. \hbar -curve for the acquired solution $u(x, t)$ versus \hbar for the considered Problem 4.1 when (i) $n = 1$ and (ii) $n = 2$ when $t = 0.01, x = 2.5$ for distinct values of α .

In the following table, (Table 1) we present comparisons of the 3rd and 6th order ARA-HTM solutions with HPTM [30] in terms of absolute error values for Problem 4.1 at $\hbar = -1, \alpha = 1$ and $n = 1$.

x	t	$u_{HPTM}^{(3)}(x, t)[14]$	$u_{ARA-HTM}^{(3)}(x, t)$	$u_{HPTM}^{(6)}(x, t)[14]$	$u_{ARA-HATM}^{(6)}(x, t)$
-6	0	0	0	0	0
	0.1	1.01250×10^{-8}	1.26493×10^{-8}	2.00000×10^{-12}	5.85415×10^{-14}
	0.2	1.58853×10^{-7}	1.99124×10^{-7}	8.00000×10^{-12}	7.37493×10^{-12}
	0.3	7.88790×10^{-7}	9.92063×10^{-7}	1.0300×10^{-10}	1.24008×10^{-10}
	0.4	2.44582×10^{-6}	3.08642×10^{-6}	7.66000×10^{-10}	9.14495×10^{-10}
	0.5	5.85975×10^{-7}	7.41928×10^{-6}	3.61500×10^{-9}	4.29356×10^{-9}

	0	0	0	0	0
6	0.1	1.43062×10^{-6}	1.30780×10^{-8}	1.41911×10^{-6}	6.05531×10^{-14}
	0.2	5.64584×10^{-6}	2.12857×10^{-7}	5.55361×10^{-6}	7.88358×10^{-12}
	0.3	1.25341×10^{-5}	1.09649×10^{-6}	1.22222×10^{-5}	1.37061×10^{-10}
	0.4	2.19832×10^{-5}	3.52734×10^{-6}	2.12426×10^{-5}	1.04514×10^{-9}
	0.5	3.38845×10^{-5}	8.76824×10^{-6}	3.24352×10^{-5}	5.07421×10^{-9}
8	0	0	0	0	0
	0.1	3.10937×10^{-9}	3.09039×10^{-9}	1.89934×10^{-12}	6.02791×10^{-15}
	0.2	5.00750×10^{-8}	5.00801×10^{-8}	4.34135×10^{-11}	7.8252×10^{-13}
	0.3	2.56853×10^{-7}	2.56823×10^{-7}	4.34570×10^{-11}	1.35434×10^{-11}
	0.4	8.22400×10^{-7}	8.22368×10^{-7}	1.34375×10^{-10}	1.02796×10^{-10}
	0.5	2.03447×10^{-6}	2.03451×10^{-6}	4.63377×10^{-10}	4.96705×10^{-10}

Example 4.2.

Consider the nonlinear time-fractional fifth-order KdV equation cited in Eq.(4)

$$D_t^\alpha u(x, t) + uu_x - uu_{xxx} + u_{xxxxx} = 0, \quad (31)$$

with initial conditions

$$u(x, 0) = e^x. \quad (32)$$

Introduce ARA transform in Eq.(31) along with the starting solution in Eq.(32), leads to

$$\mathcal{G}_t[u(x, t)] - \frac{e^x}{s} + \frac{1}{s^\alpha} \mathcal{G}_t \left\{ u \frac{\partial u}{\partial x} - u \frac{\partial^3 u}{\partial x^3} + \frac{\partial^5 u}{\partial x^5} \right\} = 0. \quad (33)$$

The nonlinear operator N is defined as follows

$$N[\varphi(x, t; q)] = \mathcal{G}_t[\varphi(x, t; q)] - \frac{e^x}{s} + \frac{1}{s^\alpha} \mathcal{G}_t \left\{ \varphi(x, t; q) \frac{\partial \varphi(x, t; q)}{\partial x} - \varphi(x, t; q) \frac{\partial^3 \varphi(x, t; q)}{\partial x^3} + \frac{\partial^5 \varphi(x, t; q)}{\partial x^5} \right\}. \quad (34)$$

The m^{th} order deformation equation is

$$\mathcal{G}_t[u_m(x, t) - K_m u_{m-1}(x, t)] = \hbar \mathfrak{R}_m[\vec{u}_{m-1}], \quad (35)$$

where

$$\begin{aligned} \mathfrak{R}_m[\vec{u}_{m-1}] &= \mathcal{G}_t[u(x, t)] - \left(1 - \frac{K_m}{n}\right) \left\{ \frac{e^x}{s} \right\} \\ &+ \frac{1}{s^\alpha} \mathcal{G}_t \left\{ \sum_{i=0}^{m-1} u_i \frac{\partial u_{m-1-i}}{\partial x} - \sum_{i=0}^{m-1} u_i \frac{\partial^3 u_{m-1-i}}{\partial x^3} + \frac{\partial^5 u_{m-1}}{\partial x^5} \right\}. \end{aligned} \quad (36)$$

When treated with inverse ARA transform with Eq.(36), we get

$$u_m(x, t) = K_m u(x, t) + \hbar \mathcal{G}_t^{-1} \{ \mathfrak{R}_m[\vec{u}_{m-1}] \}. \quad (37)$$

Solving the above equations consistently gives

$$u_0(x, t) = e^x,$$

$$u_1(x, t) = \frac{\hbar t^\alpha e^x}{\Gamma[\alpha+1]},$$

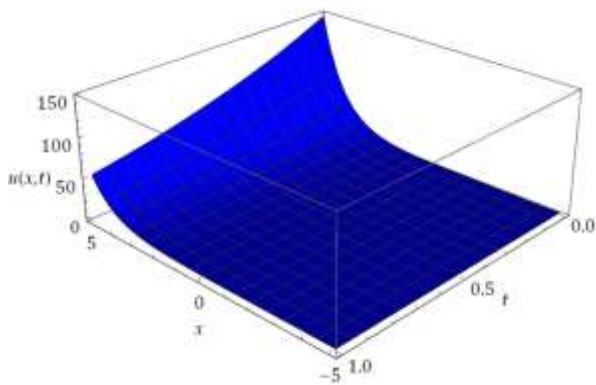
$$u_2(x, t) = \frac{(n+\hbar)\hbar t^\alpha e^x}{\Gamma[\alpha+1]} + \frac{e^x t^{2\alpha} \hbar^2}{\Gamma[2\alpha+1]},$$

$$u_3(x, t) = \frac{(n+\hbar)^2 \hbar t^\alpha e^x}{\Gamma[\alpha+1]} + \frac{(n+\hbar)e^x t^{2\alpha} \hbar^2}{\Gamma[2\alpha+1]} + \frac{e^x t^{3\alpha} \hbar^3}{\Gamma[3\alpha+1]},$$

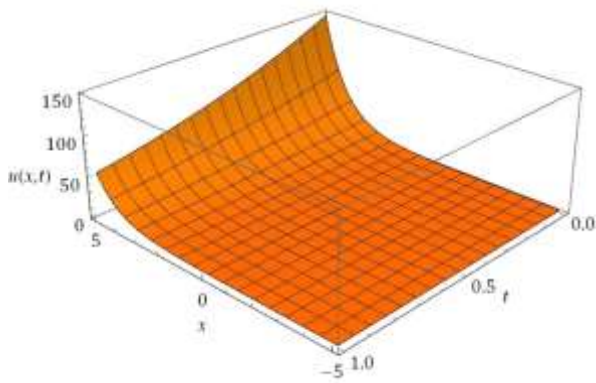
⋮

Finally, after getting further iterative terms, the essential series solution of Eq.(31) is presented by

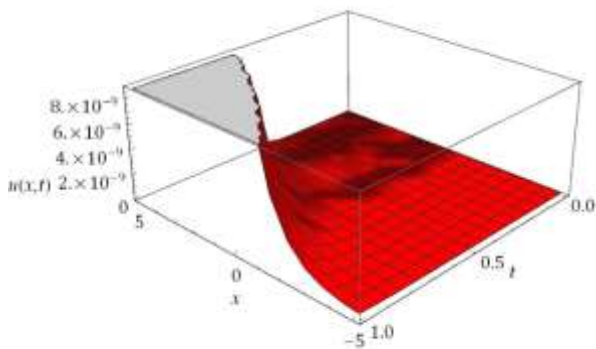
$$u(x, t) = u_0(x, t) + \sum_{m=1}^{\infty} u_m(x, t) \left(\frac{1}{n}\right)^m.$$
 Taking $n = 1, \hbar = -1$ and $\alpha = 1$, then the solution we get is in the form $\sum_{m=1}^N u_m(x, t) \left(\frac{1}{n}\right)^m$, converges to the exact solution $u(x, t) = e^{x-t}$ of the Eq.(31) as $N \rightarrow \infty$. (38)



(a)



(b)



(c)

Figure 4. 3D plots of solution surfaces indicating ARA-HTM solution, the exact solution, and an approximate error solution, respectively ((a), (b) & (c)) at $\alpha = 1, n = 1$ and $\hbar = -1$ for Problem 4.2.

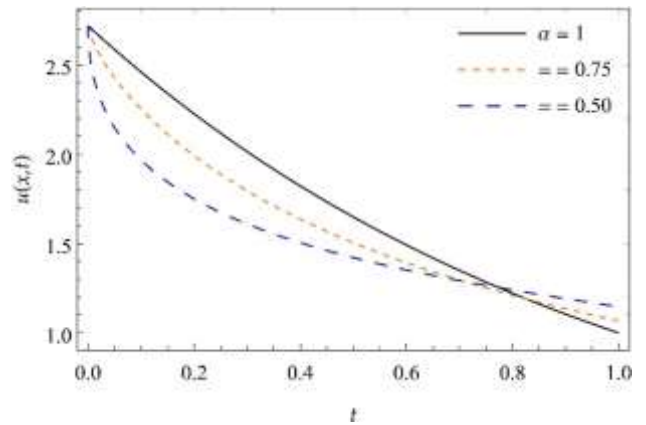
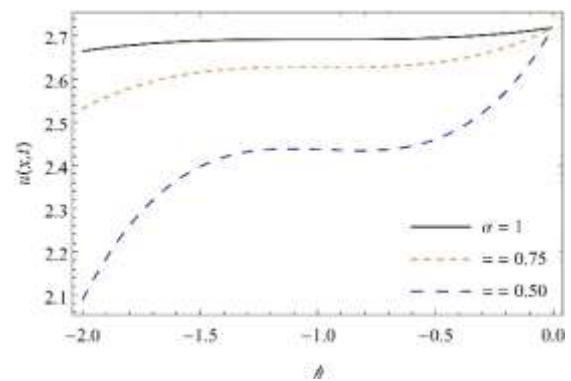
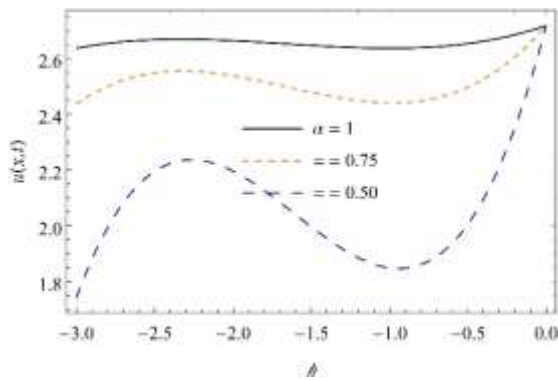


Figure 5. $u(x, t)$ versus t for Problem 4.2 at $\hbar = -1, x = 5$ and $n = 1$ for distinct values of α .



(i)



(ii)

Figure 6. h -curve for acquired solution $u(x, t)$ for Problem 4.2 when (i) $n = 1$ and (ii) $n = 2$ when $x = 1$ and $t = 0.001$ for distinct values of α .

In the following table, (Table 2) we present the 3rd to 6th-order approximations of the obtained ARA-HTM series solution for Problem 4.2 at $h = -1, \alpha = 1$ and $n = 1$.

x	t	$u_{ARA-HTM}^{(3)}(x, t)$	$u_{ARA-HTM}^{(4)}(x, t)$	$u_{ARA-HTM}^{(5)}(x, t)$	$u_{ARA-HTM}^{(6)}(x, t)$
-5	0	0	0	0	0
	0.1	2.75225×10^{-8}	5.52269×10^{-10}	9.22623×10^{-12}	1.32034×10^{-13}
	0.2	4.31811×10^{-7}	1.73856×10^{-8}	5.82235×10^{-10}	1.66938×10^{-11}
	0.3	2.14415×10^{-6}	1.29903×10^{-7}	6.54040×10^{-9}	2.81769×10^{-10}
	0.4	6.64842×10^{-6}	5.38726×10^{-7}	3.62459×10^{-8}	2.08553×10^{-9}
	0.5	1.59285×10^{-5}	1.61828×10^{-6}	1.36397×10^{-7}	9.82624×10^{-9}
5	0	0	0	0	0
	0.1	6.06224×10^{-4}	1.21645×10^{-5}	2.03221×10^{-7}	2.90825×10^{-9}
	0.2	9.51127×10^{-3}	3.82944×10^{-4}	1.28246×10^{-5}	3.67705×10^{-7}
	0.3	4.72281×10^{-2}	2.8613×10^{-3}	1.44062×10^{-4}	6.20638×10^{-6}
	0.4	1.46441×10^{-1}	1.18662×10^{-2}	7.98369×10^{-4}	4.59368×10^{-5}
	0.5	3.50848×10^{-1}	3.56449×10^{-2}	3.00433×10^{-3}	2.16437×10^{-4}

Example 4.3. Consider the time-fractional fifth-order KdV equation

$$D_t^\alpha u(x, t) + uu_x + u_{xxx} - u_{xxxxx} = 0, \quad (39)$$

with the initial condition

$$u(x, 0) = \frac{105}{169} \operatorname{sech}^4 \left(\frac{x-k}{2\sqrt{13}} \right). \quad (40)$$

By performing ARA transform on Equation (39) and then considering Eq.(40), we get

$$\mathcal{G}_t[u(x, t)] - \frac{1}{s} \left(\frac{105}{169} \operatorname{sech}^4 \left(\frac{x-k}{2\sqrt{13}} \right) \right) + \frac{1}{s^\alpha} \mathcal{G}_t \left\{ u \frac{\partial u}{\partial x} + \frac{\partial^3 u}{\partial x^3} - \frac{\partial^5 u}{\partial x^5} \right\} = 0. \quad (41)$$

The nonlinear operator N is defined as follows

$$N[\varphi(x, t; q)] = \mathcal{G}_t[\varphi(x, t; q)] - \frac{1}{s} \left\{ \frac{105}{169} \operatorname{sech}^4 \left(\frac{x-k}{2\sqrt{13}} \right) \right\} + \frac{1}{s^\alpha} \mathcal{G}_t \left\{ \varphi(x, t; q) \frac{\partial \varphi(x, t; q)}{\partial x} + \frac{\partial^3 \varphi(x, t; q)}{\partial x^3} - \frac{\partial^5 \varphi(x, t; q)}{\partial x^5} \right\}. \quad (42)$$

The m^{th} order deformation equation is

$$\mathcal{G}_t[u_m(x, t) - K_m u_{m-1}(x, t)] = \hbar \mathfrak{R}_m[\vec{u}_{m-1}], \quad (43)$$

where

$$\begin{aligned} \mathfrak{R}_m[\vec{u}_{m-1}] = & \mathcal{G}_t[u(x, t)] - \left(1 - \frac{K_m}{n}\right) \frac{1}{s} \left\{ \frac{105}{169} \operatorname{sech}^4\left(\frac{x-k}{2\sqrt{13}}\right) \right\} \\ & + \frac{1}{s^\alpha} \mathcal{G}_t \left\{ \sum_{i=0}^{m-1} u_i \frac{\partial u_{m-1-i}}{\partial x} + \frac{\partial^3 u_{m-1-i}}{\partial x^3} - \frac{\partial^5 u_{m-1-i}}{\partial x^5} \right\}. \end{aligned} \quad (44)$$

By enforcing the inverse ARA transform with Eq.(43), we get

$$u_m(x, t) = K_m u(x, t) + \hbar \mathcal{G}_t^{-1} \{ \mathfrak{R}_m[\vec{u}_{m-1}] \}. \quad (45)$$

Solving the above equations consistently gives

$$u_0(x, t) = \frac{105}{169} \operatorname{sech}^4\left(\frac{x-k}{2\sqrt{13}}\right),$$

$$u_1(x, t) = -\frac{7560\hbar t^\alpha}{28561\sqrt{13}\Gamma[\alpha+1]} \operatorname{sech}^4\left(\frac{x-k}{2\sqrt{13}}\right) \tanh\left(\frac{x-k}{2\sqrt{13}}\right),$$

$$u_2(x, t) = -\frac{(n+\hbar)7560\hbar t^\alpha}{28561\sqrt{13}\Gamma[\alpha+1]} \operatorname{sech}^4\left(\frac{x-k}{2\sqrt{13}}\right) \tanh\left(\frac{x-k}{2\sqrt{13}}\right) + \frac{136080t^{2\alpha}\hbar^2 \operatorname{sech}^6\left(\frac{x-k}{2\sqrt{13}}\right)}{62748517\Gamma[1+2\alpha]} \left(-3 + 2\cosh\left(\frac{x-k}{\sqrt{13}}\right)\right),$$

$$u_3(x, t) = -\frac{7560(n+\hbar)^2\hbar t^\alpha}{28561\sqrt{13}\Gamma[\alpha+1]} \operatorname{sech}^4\left(\frac{x-k}{2\sqrt{13}}\right) \tanh\left(\frac{x-k}{2\sqrt{13}}\right) + \frac{(n+\hbar)136080t^{2\alpha}\hbar^2 \operatorname{sech}^6\left(\frac{x-k}{2\sqrt{13}}\right)}{62748517\Gamma[2\alpha+1]} \left(-3 + 2\cosh\left(\frac{x-k}{\sqrt{13}}\right)\right)$$

$$+ \frac{204120t^{3\alpha}\hbar^3}{10604499373\sqrt{13}\Gamma[1+\alpha]^2\Gamma[1+3\alpha]} \operatorname{sech}^{10}\left(\frac{x-k}{2\sqrt{13}}\right) \tanh\left(\frac{x-k}{2\sqrt{13}}\right)$$

$$\times \left((-765 + 650\cosh\left(\frac{x-k}{\sqrt{13}}\right)) + 9\cosh\left(\frac{2(x-k)}{\sqrt{13}}\right)\Gamma[1+\alpha]^2 - 6\cosh\left(\frac{3(x-k)}{\sqrt{13}}\right)\right)\Gamma[1+\alpha]^2$$

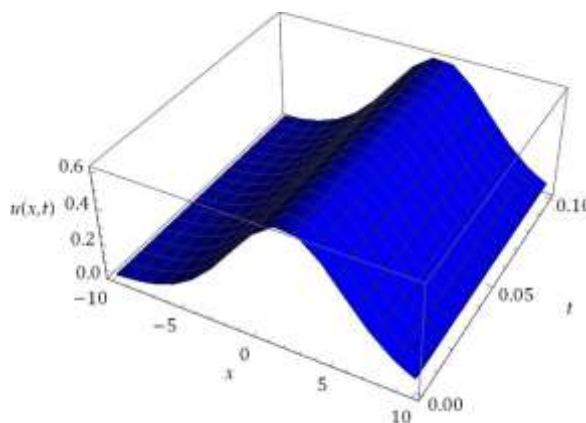
$$+ 140\left(3 - 2\cosh\left(\frac{x-k}{\sqrt{13}}\right)\right)\Gamma[1+2\alpha],$$

⋮

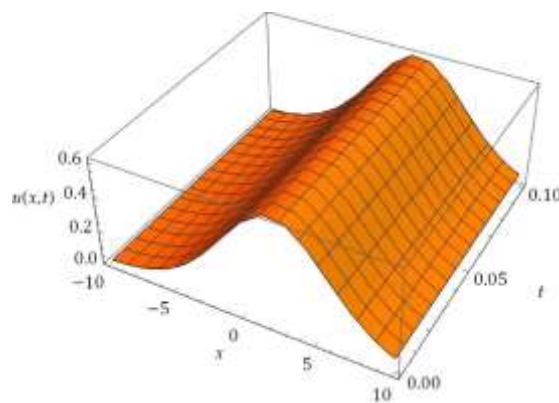
Finally, after getting further iterative terms, the essential series solution of Equation (39) is presented by

$$u(x, t) = u_0(x, t) + \sum_{m=1}^{\infty} u_m(x, t) \left(\frac{1}{n}\right)^m. \quad (46)$$

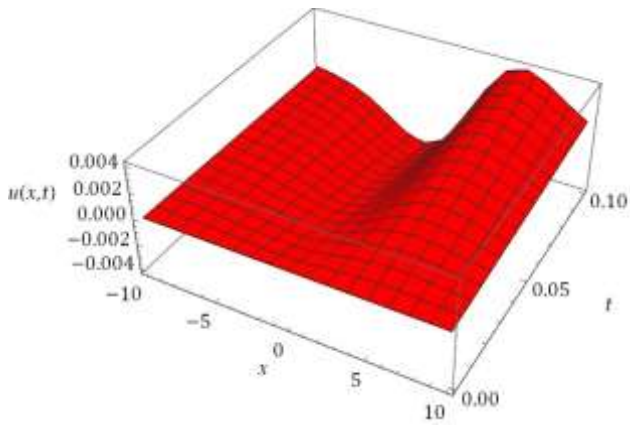
If we take $\hbar = -1, \alpha = 1$ and $n = 1$, then the secured solution $\sum_{m=1}^N u_m(x, t) \left(\frac{1}{n}\right)^m$, converges to the exact solution $u(x, t) = \frac{105}{169} \operatorname{sech}^4\left(\frac{1}{2\sqrt{13}}\left(x + \frac{36t}{169} - k\right)\right)$ of the Eq.(39), as $N \rightarrow \infty$.



(a)

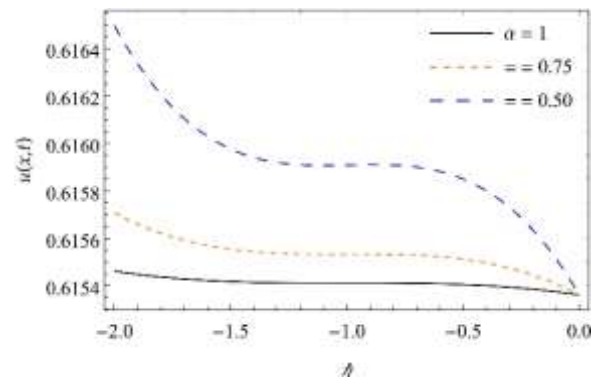


(b)

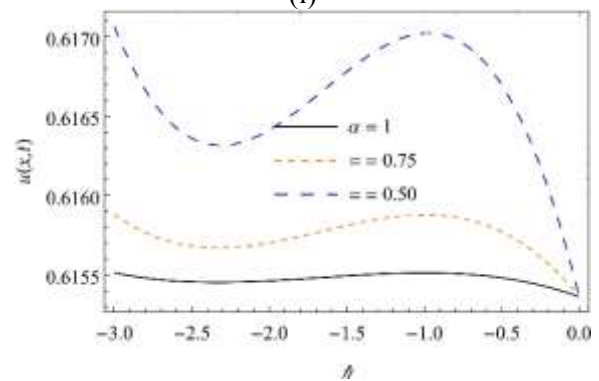


(c)

Figure7. (a) 3D plot for ARA-HTM solution, (b) surface of exact solution, (c) approximate error solution surface, at $\hbar = -1$, $a = 4$, $n = 1$ and $\alpha = 1$.



(i)



(ii)

Figure 9. \hbar -curve for acquired solution $u(x, t)$ for Problem 4.3 when (i) $n = 1$ and (ii) $n = 2$ when $x = 2.5, k = 2$ and $t = 0.01$ for distinct values of α .

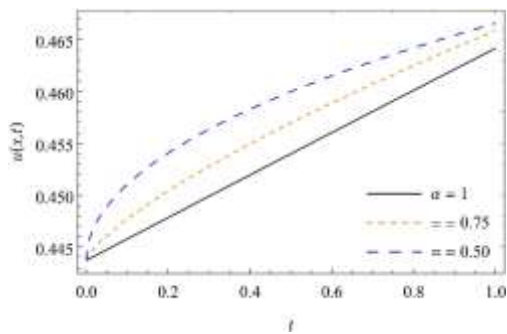


Figure8. $u(x, t)$ versus t for the contemplated Problem 4.3 at $\hbar = -1, x = 5, k = 2$ and $n = 1$ for distinct values of α .

In the following table, (Table 3) we present a numerical study of the achieved results in terms of absolute error for Problem 4.3 at $\hbar = -1, \alpha = 1$ and $n = 1$ and different values of x and t .

x	t	$u_{ARA-HTM}^{(2)}(x, t)$	$u_{ARA-HTM}^{(3)}(x, t)$
	0	0	0
-5	0.1	2.11915×10^{-3}	2.11916×10^{-3}
	0.2	4.23833×10^{-3}	4.23836×10^{-3}

	0.3	6.35756×10^{-3}	6.35768×10^{-3}
	0.4	8.47686×10^{-3}	8.47714×10^{-3}
	0.5	1.05963×10^{-2}	1.05968×10^{-2}
5	0	0	0
	0.1	4.12712×10^{-3}	4.12709×10^{-3}
	0.2	8.25406×10^{-3}	8.25384×10^{-3}
	0.3	1.23807×10^{-2}	1.23799×10^{-2}
	0.4	1.65068×10^{-2}	1.65050×10^{-2}
	0.5	2.06322×10^{-2}	2.06287×10^{-2}
10	0	0	0
	0.1	1.47761×10^{-3}	1.47762×10^{-3}
	0.2	2.95525×10^{-3}	2.95530×10^{-3}
	0.3	4.43297×10^{-3}	4.43312×10^{-3}
	0.4	5.91079×10^{-3}	5.91116×10^{-3}
	0.5	7.38874×10^{-3}	7.38947×10^{-3}

5 Numerical results and discussion

This portion of the article provides an incorporation of numerical simulations of the investigated problem that show the validity and effectiveness of the considered scheme q-HATM. Moreover, incorporated a detailed description of the graphical solutions that were found. The secured results are very satisfying and in good fit with the exact solutions to the contemplated problem. The comparison of 3D surface plots of the obtained approximate solution and the exact solution along with their absolute error solutions is presented in Figure 1. We can see the accuracy of the obtained approximated solution of Problem 4.1 in Figure 1(c) with the least error values. The nature of the obtained solutions for different fractional order α as we move along time t is cited in figure 2. We can see the variation in the solution affected by different fractional orders. Figure 3 cites the plot of solution curves for distinct fractional orders, which gives the precise range of convergence control parameter h to achieve the convergence. The figure shows that we can choose h values between -1.4 to -0.4 for the faster convergence of the approximated solution towards the exact solution. The convergence of the obtained solution is achieved by considering $h = -1$ in this work. Table 1 depicts the comparison of secured results with the homotopy perturbation transform method (HPTM) in terms of absolute error values with $h = -1, n = 1$ and $\alpha = 1$. The calculations of table 1 are carried out by taking $x = -6, 6$ and 8 with the time interval $[0, 0.5]$. Surface plots of the q-HATM solution, the exact solution,

and the approximated error solution for Example 4.2 are cited in Figure 4. The 2D plot of the obtained solution of Problem 4.2 with respect to time t for different fractional order α is cited in figure 5. We can observe that the solution curve leads to different consequences for different fractional orders α . The performance of n with h in an accomplished outcome of the provided method is shown in figure 6. The solution of Problem 4.2 in terms of an absolute error from 3rd-order to 6th-order approximations is given in Table 2. That shows we can achieve better results by increasing the number of iterations. Figures 7(a) and 7(b) explore the 3D surfaces of the ARA-HTM solution and the exact solution of Problem 4.3. The approximated absolute error solution of Problem 4.3 is cited in Figure 7(c). The fractional behaviour of the considered nonlinear time-fractional fifth-order KdV equation over time t for distinct fractional order α is plotted in figure 8. To attain the precise range of convergence control parameters to have a faster rate of convergence to the exact solution, we have plotted Figure 9. Table 3 cites the approximated absolute error values of Problem 4.3 for different values of x and t .

The 3D plots presented in Figures (1), (4) and (7) describe the wavy nature of the considered nonlinear KdV equations. For the purpose of accuracy we can consider the plots for the fractional/classical order $\alpha = 1$, there we can see the close association of the ARA-HTM solution with the exact solution. The physical interpretation of the considered fractional problems are well described by the fractional orders $\alpha = 0.75$ and $\alpha =$

0.50 due to their feature of memory effect. From the 2D plots one can see the considered value for the convergence control parameter $\hbar = -1$ works for all the fractional orders.

From all figures, we can observe that the hired fractional operator in the considered model exemplifies some interesting consequences and it authorizes the model to noticeably defend time and history behaviour. Moreover, the illustrated numerical simulations confirm the applicability as well as the accuracy of the considered solution procedure, and, we prove that we go close to the exact solution as we increase the number of iterations. Some relevant study can be found in [39].

6 Conclusion

In the present work, the investigation of the time-fractional nonlinear fifth-order KdV equation is carried out using an analytical algorithm called ARA-HTM. We discussed three nonlinear problems to testify to the ability of the projected method to handle complex nonlinear problems. The results are highly pleasing and attest to the effectiveness of the strategy under consideration. The fractional operator considered in the present framework gives more degrees of freedom and incorporates the nonlocal effect in the projected model. The innovative aspect of this approach is its straightforward process, which enables us to arrive at a solution quickly and identifies a substantial region of convergence. The rate of convergence of the obtained series solution to the exact solution is accelerated with the help of optimal values of the convergence control parameter \hbar . The obtained numerical simulations guarantee the results with higher accuracy. Tables provide great satisfactory results when comparing with homotopy perturbation transform method (HPTM). As a future research direction, readers can use the hybrid methodologies merging with our projected scheme to achieve better consequences. Finally, we claim that our proposed technique is incredibly dependable and can be applied to large study classifications relating to fractional-order nonlinear scientific methods.

Acknowledgement:

The author expresses her gratitude to the dear unknown referees and the editor for their helpful suggestions, which improved the final version of this paper.

References:

- [1] P. Veerasha, D. G. Prakasha, A. H. Abdel-Aty, H. Singh, E. E. Mahmoud, S. Kumar, An efficient approach for fractional nonlinear chaotic model with Mittag-Leffler law, *Journal of King Saud University-Science*, 2021;33(2):101347.
- [2] R. Hilfer, *Applications of fractional calculus in physics*, World Scientific, Singapore, 2000.
- [3] M. A. Abdou, An analytical method for space-time fractional nonlinear differential equations arising in plasma physics, *Journal of Ocean Engineering and Science*, 2017;2:288-292.
- [4] M. Al-Smadi, O. A. Arqub, S. Momani, Numerical computations of coupled fractional resonant Schrödinger equations arising in quantum mechanics under conformable fractional derivative sense, *Physica Scripta*, 2020;95(7):075218.
- [5] S. S. Chen, B. Tian, Y. Sun, C. R. Zhang, Generalized Darboux transformations, rogue waves, and modulation instability for the coherently coupled nonlinear Schrödinger equations in nonlinear optics, *Annalen der Physik*, 2019;531(8):1900011.
- [6] R. Saadeh, A Reliable Algorithm for Solving System of Multi-Pantograph Equations, *WSEAS transactions on mathematics*, 2022; 2022 (DOI 10.37394/23206.2022.21.91).
- [7] D. Kumar, C. Park, N. Tamanna, G. C. Paul, M. S. Osman, Dynamics of two-mode Sawada-Kotera equation: Mathematical and graphical analysis of its dual-wave solutions, *Results in Physics*, 2020;19:103581.
- [8] M. Bilal, A. R. Seadawy, M. Younis, S. T. R. Rizvi, H. Zahed, Dispersive of propagation wave solutions to unidirectional shallow water wave Dullin–Gottwald–Holm system and modulation instability analysis, *Mathematical Methods in the Applied Sciences*, 2021;44(5):4094-4104.
- [9] A. R. Seadawy, A. Ali, W. A. Albarakati, Analytical wave solutions of the (2+ 1)-dimensional first integro-differential Kadomtsev-Petviashvili hierarchy equation by using modified mathematical methods, *Results in Physics*, 2019;15:102775.
- [10] R. A. Shahein, A. R. Seadawy, Bifurcation analysis of KP and modified KP equations in an unmagnetized dust plasma with nonthermal distributed multi-temperatures ions, *Indian Journal of Physics*, 2019;93(7):941-949.

- [11] I. Ali, A. R. Seadawy, S. T. R. Rizvi, M. Younis, K. Ali, Conserved quantities along with Painleve analysis and Optical solitons for the nonlinear dynamics of Heisenberg ferromagnetic spin chains model, *International Journal of Modern Physics B*, 2020;34(30):2050283.
- [12] K. K. Ali, M. A. Abd El Salam, E. M. Mohamed, B. Samet, S. Kumar, M. S. Osman, Numerical solution for generalized nonlinear fractional integro-differential equations with linear functional arguments using Chebyshev series, *Advances in Difference Equations*, 2020;2020(1):1-23.
- [13] M. A. Akbar, A. M. Wazwaz, F. Mahmud, D. Baleanu, R. Roy, H. K. Barman, ... M. S. Osman, Dynamical behavior of solitons of the perturbed nonlinear Schrödinger equation and microtubules through the generalized Kudryashov scheme, *Results in Physics*, 2022;43:106079.
- [14] Y. Saliou, S. Abbagari, A. Houwe, M. S. Osman, D. S. Yamigno, K. T. Crépin, M. Inc, W-shape bright and several other solutions to the $(3+ 1)$ -dimensional nonlinear evolution equations, *Modern Physics Letters B*, 2021;35(30):2150468.
- [15] M. S. Osman, K. U. Tariq, A. Bekir, A. Elmoasry, N. S. Elazab, M. Younis, M. Abdel-Aty, Investigation of soliton solutions with different wave structures to the $(2+ 1)$ -dimensional Heisenberg ferromagnetic spin chain equation, *Communications in Theoretical Physics*, 2020;72(3):035002.
- [16] S. Malik, H. Almusawa, S. Kumar, A. M. Wazwaz, M. S. Osman, A $(2+ 1)$ -dimensional Kadomtsev–Petviashvili equation with competing dispersion effect: Painlevé analysis, dynamical behavior and invariant solutions, *Results in Physics*, 2021;23:104043.
- [17] I. Siddique, M. M. Jaradat, A. Zafar, K. B. Mehdi, M. S. Osman, Exact traveling wave solutions for two prolific conformable M-Fractional differential equations via three diverse approaches, *Results in Physics*, 2021;28:104557.
- [18] D. J. Korteweg, G. de Vries, On the change of form of long waves advancing in a rectangular canal and on a new type of long stationary waves, *Philosophical Magazine* 1895;39(5):422-43.
- [19] J. Singh, D. Kumar, S. Kumar, A reliable algorithm for solving discontinued problems arising in nanotechnology, *Scientia Iranica* 2013;20(3):1059-62.
- [20] R. Saadeh, O. Ala'yed, A. Qazza, Analytical Solution of Coupled Hirota–Satsuma and KdV Equations. *Fractal and Fractional* 2022;6(12):694.
- [21] M. Almazmumy, F. A. Hendi, H. O. Bakoda, H. Alzumi. Recent Modification of Adomian Decomposition Method for initial value problem in ordinary differential equations. *Am. J. Comput. Math.* 2012;2:228–34.
- [22] H. O. Bakodah. Modified Adomian decomposition method for the generalized fifth order KdV equations. *American Journal of Computational Mathematics*, 2013;3(1):53.
- [23] Y. Khan. An effective modification of the Laplace decomposition method for nonlinear equations. *Int. J. Nonlin. Sci. Numer. Simul.* 2009;10:1373–6.
- [24] A. Qazza, R. Saadeh, R. (2023). On the Analytical Solution of Fractional SIR Epidemic Model. *Applied Computational Intelligence and Soft Computing*, 2023..
- [25] Saadeh, R., Abbes, A., Al-Husban, A., Ouannas, A., & Grassi, G. (2023). The Fractional Discrete Predator–Prey Model: Chaos, Control and Synchronization. *Fractal and Fractional*, 7(2), 120..
- [26] R. Hirota. Exact solution of the Korteweg-de Vries equation for multiple collisions of solitons. *Phys. Rev. Lett.* 1971;27:1192–4.
- [27] Al-Husban, A., Djenina, N., Saadeh, R., Ouannas, A., & Grassi, G. (2023). A New Incommensurate Fractional-Order COVID 19: Modelling and Dynamical Analysis. *Mathematics*, 11(3), 555..
- [28] G. C. Wu, J.H. He, Fractional calculus of variations in fractal spacetime, *Nonlin. Sci. Lett. A* 2010;3:281–7.
- [29] A. M. Wazwaz, The extended tanh method for new solitons solutions for many forms of the fifth-order KdV equations, *Applied Mathematics and Computation*, 2007;184(2): 1002-14.
- [30] H. Jafari, M. A. Firoozjaee. Homotopy analysis method for solving KdV equations. *Surveys Math. Applicat.* 2010;5:89–98.
- [31] R. Saadeh, A. Qazza, A. Burqan, On the Double ARA-Sumudu transform and its applications. *Mathematics* 2022, 10(15), 2581.
- [32] A. Qazza, A. Burqan, R. Saadeh, Application of ARA-Residual Power Series Method in Solving Systems of Fractional Differential Equations. *Mathematical Problems in Engineering* 2022, 2022.

- [33] A. Qazza, R. Saadeh, E. Salah, Solving fractional partial differential equations via a new scheme. AIMS Mathematics 2023, 8(3), 5318-5337.
- [34] Saadeh, R., Qazza, A., & Burqan, A. (2020). A new integral transform: ARA transform and its properties and applications. Symmetry, 12(6), 925.
- [35] Qazza, A., Burqan, A., & Saadeh, R. (2021). A new attractive method in solving families of fractional differential equations by a new transform. Mathematics, 9(23), 3039.
- [36] Saadeh, R. (2022). Applications of double ARA integral transform. Computation, 10(12), 216.
- [37] Saadeh, R. (2023). Application of the ARA Method in Solving Integro-Differential Equations in Two Dimensions. Computation, 11(1), 4.
- [38] Kawahara (1972), T. Oscillatory solitary waves in dispersive media, Journal of the Physical Society of Japan, Volume 33, Issue 1, 1972, Pages 260-264
- [39] Ivan V. Kazachkov (2021), Modern Status of the Parametric Excitation of Oscillations in Film Flows and Granulation for Amorphous Materials' Production, MOLECULAR SCIENCES AND APPLICATIONS, pp.58-67, Volume 1, 2021, DOI: 10.37394/232023.2021.1.10,

Sources of Funding for Research Presented in a Scientific Article or Scientific Article Itself
Report potential sources of funding if there is any

Creative Commons Attribution License 4.0 (Attribution 4.0 International, CC BY 4.0)

This article is published under the terms of the Creative Commons Attribution License 4.0

https://creativecommons.org/licenses/by/4.0/deed.en_US